

Alternative Solution Regarding Problems of Adaptive Observer Compensating Parameters Uncertainties for Sensorless Induction Motor Drives

Jiahao Chen, *Member, IEEE*, Jin Huang

Abstract—This paper first shows that the advanced high gain adaptive observer (AO) is able to estimate both speed and resistances during speed transients. However, it is also found that high gain AO based resistances estimation begins to diverge as the operating speed becomes higher. The problem is due to the fact that the model sensitivity of speed is much higher than that of resistances at high speeds. As a result, this paper claims that the high gain AO is not generally a good option to compensate parameters uncertainties in sensorless induction motor drives for all working conditions. As an alternative, this paper proposes a scheme which not only has the potential of high dynamic performance but also avoids the aforementioned ‘sensitivity problem’. Besides, interesting topics, such as speed-dependent resistance estimation, sensorless inertia identification, slow speed reversal test, and reduced-order natural speed observer, are all covered in this paper. Effective experiment verifies the feasibility of the proposed scheme, which is deemed to have potentials for practical applications.

Index Terms—speed-dependent estimation, sensorless inertia identification, slow reversal, natural observer.

I. INTRODUCTION

A. Literature Review

SINCE the review paper by Holtz [1], the research focuses of sensorless induction motor (IM) drives have been shifted on two ensuing tasks. One is to solve the problem of regeneration-mode instability, while the other is to overcome the problem of parameters variation.

On the one hand, an overview of parameter estimation methods can be found in [2], in which most methods attempt to identify a single motor parameter. Among them, stator resistance is crucial for low speed stability of sensorless drive, while the rotor resistance is often required for flux orientation. Therefore, it is more reasonable to identify both stator and rotor resistances, especially at low speeds. This topic is later covered in [3].

This work was supported in part by the National Key Basic Research Program of China (973 Project) under Grant 2013CB035604 and in part by the National Natural Science Foundation of China under Grant 51690182.

J. Chen and J. Huang are with the College of Electrical Engineering, Zhejiang University, Hangzhou 310027, China (e-mail: ho-rychen@qq.com).

On the other hand, there are two ways to analyze and attack the regeneration-mode instability problem. In the literature, it is popular to consider speed as a constant motor parameter, making rotor fluxes the regressor of speed. Since measurements of rotor currents/fluxes are unavailable for squirrel-cage IMs and the adaptive observer (AO) design technique for a system with unknown regressor is unclear at the time, it is shown to be impossible to construct globally stable speed-AO for IMs [4]. Simplified or approximated speed estimation methods suffer from the unstable behaviors during low speed regenerating operation. Therefore, efforts are put to attain local stability instead, and those stabilization techniques are surveyed in [5].

As a second way to deal with the regeneration-mode instability problem, there are researches aiming at finding a Lyapunov function for the speed estimation. To date, a lot of stable designs of sensorless IM control have been seen in the literature. The key step usually involves a state transformation. There are designs with observer stability analysis [6]–[13] as well as designs with observer-controller stability analysis [14]–[21]. One distinct difference is that reference values can be exploited in the adaptive design for the latter [15]–[18].

In addition, some recent works focus on further extending the speed range of the sensorless IM drive to high speeds [22], to low speeds [23], and even towards zero frequency operation [24]. Besides, an exclusive review for different model reference adaptive system is found in [25], among which the super-twisting algorithm based variant has drawn a lot of attention [26], [27].

B. Motivation of this Paper

It is natural to pursue a stable sensorless design with resistances adaptation, for all working conditions that include not only regenerating operation but also variable speed operation.

Low dynamic performance is expected for designs that make constant speed assumption [6], [7], [11]–[13] or neglect unmodeled dynamics [10]. Particularly, in [9], the estimated speed becomes the solution of a quadratic equation when speed varies. Others construct speed observer using the mechanical equation of IMs to attain high performance at transients [8], [15]–[21].

Also, compensating for resistances variation will improve the performance at steady state and during speed transients.

TABLE I. List of Symbols

<i>Inverse-Γ-circuit Symbols</i>	<i>Notation</i>	<i>Comment</i>
Stator resistance	r_s	3.04Ω
Rotor resistance	r_{req}	1.60Ω
Stator leakage inductance	L_σ	0.0249 H
Magnetizing inductance	L_μ	0.448 H
Stator voltage in α - β frame	u_s	$u_s = [u_{\alpha s}, u_{\beta s}]^T$
Stator current in α - β frame	i_s	$i_s = [i_{\alpha s}, i_{\beta s}]^T$
Rotor flux (linkage) in α - β frame	ψ_μ	$\psi_\mu = [\psi_{\alpha \mu}, \psi_{\beta \mu}]^T$
Rotor current in α - β frame	i_{req}	$i_{req} = L_\mu^{-1} \psi_\mu - i_s$
Stator flux (linkage) in α - β frame	ψ_s	$\psi_s = L_\sigma i_s + \psi_\mu$
<i>Other Symbols</i>	<i>Notation</i>	<i>Comment</i>
Differentiation operator	p or \cdot	$p = \frac{d}{dt}, \dot{x} = \frac{d}{dt}x$
Number of pole pairs	n_{pp}	$n_{pp} = 2$
Shaft inertia (nominal)	J_{sN}	0.017 kgm^2
Inverse mechanical time constant	μ_m	$\triangleq n_{pp}/J_s$
Load torque	T_L	-
Inverse rotor time constant	α	$\triangleq r_{req}/L_\mu$
Electrical rotor angular speed	ω	-
Synchronous angular speed	ω_ψ	-
Slip angular speed	ω_{sl}	$\triangleq \omega_\psi - \omega$
Rotor flux command modulus	ψ^*	$\triangleq m_0 + m_1 \sin(\omega_t t)$
VM based flux estimate	ψ_2	$\psi_2 = [\psi_{\alpha 2}, \psi_{\beta 2}]^T$
Output error of high gain AO	\tilde{y}	$\tilde{y} = i_s - \dot{i}_s$
High gain coefficient	ϑ	-

Particularly, difficulty is reported when extending a stable sensorless design to include stator resistance identification [12], [28], [29], unless an AO that applies for systems with nonlinear parametrization and unknown regressor is proposed [10], [13], [19]. Besides, it is analyzed in [30] that rotor resistance seen from the inverse- Γ circuit can vary abruptly as load torque and speed change in the experiment. So it is also desired to identify rotor resistance during speed transients for high performance drives.

To the authors' knowledge, so far no scheme from the literature has taken the above two aspects into account, except the one by Dib [19], [31]. Dib has proposed the high gain AO that is able to estimate speed and resistances even during speed transients, as shown in Fig. 1a.

From Fig. 1a, when $t \in [10, 35]$ s and speed is 50 rad/s, small bumps (rather than spikes) of resistances estimations can be spotted in the zoomed-in plots. This implies that the transients due to speed command changes have very limited influence on the resistances estimations while the change of speed value does cause biased resistances estimation. At $t = 50$ s, a load torque change is applied, which contradicts the model assumption $pT_L = 0$ and disturbs the estimations of ω , r_s and r_{req} . However, one observes that the norm of output error \tilde{y} grows as speed increases, which could be the very cause of the biased resistances estimations.

In Fig. 1b, the simulation continues for higher speeds. At $t = 70$ s, the speed command goes up to 100 rad/s, and as highlighted by the zoomed-in plot, the resistances estimations are slightly biased as $\|\tilde{y}\|$ increases. By intuition, one may guess that a larger tuning coefficient ϑ could reduce $\|\tilde{y}\|$. To test this thought, we set ϑ to 200 s^{-1} at $t = 150$ s. As a result, $\|\tilde{y}\|$ becomes even larger, which makes the parameters estimation accuracy even worse. At $t = 220$ s, the speed command further rises to 150 rad/s and the resistances estimations begin to slowly drift away, which causes biased

speed estimation/control. This is deemed to be a general problem of using AO to estimate both speed and resistances.

The fact that the AO based resistances estimation becomes biased at higher speeds, could be explained by the parameter sensitivity study [32]. The sensitivity of \tilde{y} w.r.t. (with respect to) speed is related to the norm of back electromotive forces, while the sensitivity of \tilde{y} w.r.t. resistances is related to the norm of currents. That is to say, as the speed gets higher, a small speed estimated error could lead to a large $\|\tilde{y}\|$. Apparently, compensating such $\|\tilde{y}\|$ via tuning estimated resistances could result in severely biased or even diverged results, given the fact that the sensitivities of resistances are very low compared to that of speed at higher speeds.

To summarize, the high gain AO is able to estimate speed and resistances during speed transients, but it also has the following disadvantages:

- (1) Motion equation based speed observation needs information about inertia. The dynamic performance of speed estimation deteriorates with a detuned inertia.
- (2) Sensitivity of rotor resistance becomes low at higher speed, which leads to speed-dependent estimation of rotor resistance.
- (3) Resistance convergence rate can not be tuned separately from the speed estimation. As a result, large oscillation in resistances estimations cannot be avoided for sudden load change.
- (4) Computational burden is heavy. There are 23 states to implement.

II. THE PROPOSED ALTERNATIVE SCHEME

As an alternative solution to high gain AO, we propose a sensorless scheme that consists of a 2nd-order voltage model (VM) based flux estimation and a 3rd-order load torque-adaptive natural speed observer. Speed observer independent parameters identifiers for stator resistance, rotor resistance and shaft inertia are also included. To this end, the VM based flux estimation is first introduced. Then, we interpret the speed observability and parameters identifiability as

- Speed is observable if the field is rotating or the speed is changing;
- Stator resistance information is indicated by the computed Joule heating loss;
- Rotor resistance information is exhibited by the changing rate of the estimated flux modulus;
- Inertia is identified from the orthogonal indicator when the speed signal is periodical.

A. Voltage Model (VM) based Flux Estimation

VM based flux estimation provides an estimate of rotor flux (denoted by ψ_2) that is free of rotor-side parameters and mechanical parameters. However, the VM of IM is critically stable, so remedies are necessary to stabilize the system [33], two of which are found simple and effective: Ohtani's method [34] and Holtz and Quan's method [35].

However, if a variable speed operation is imposed, Ohtani's method gives degenerated performance because during speed

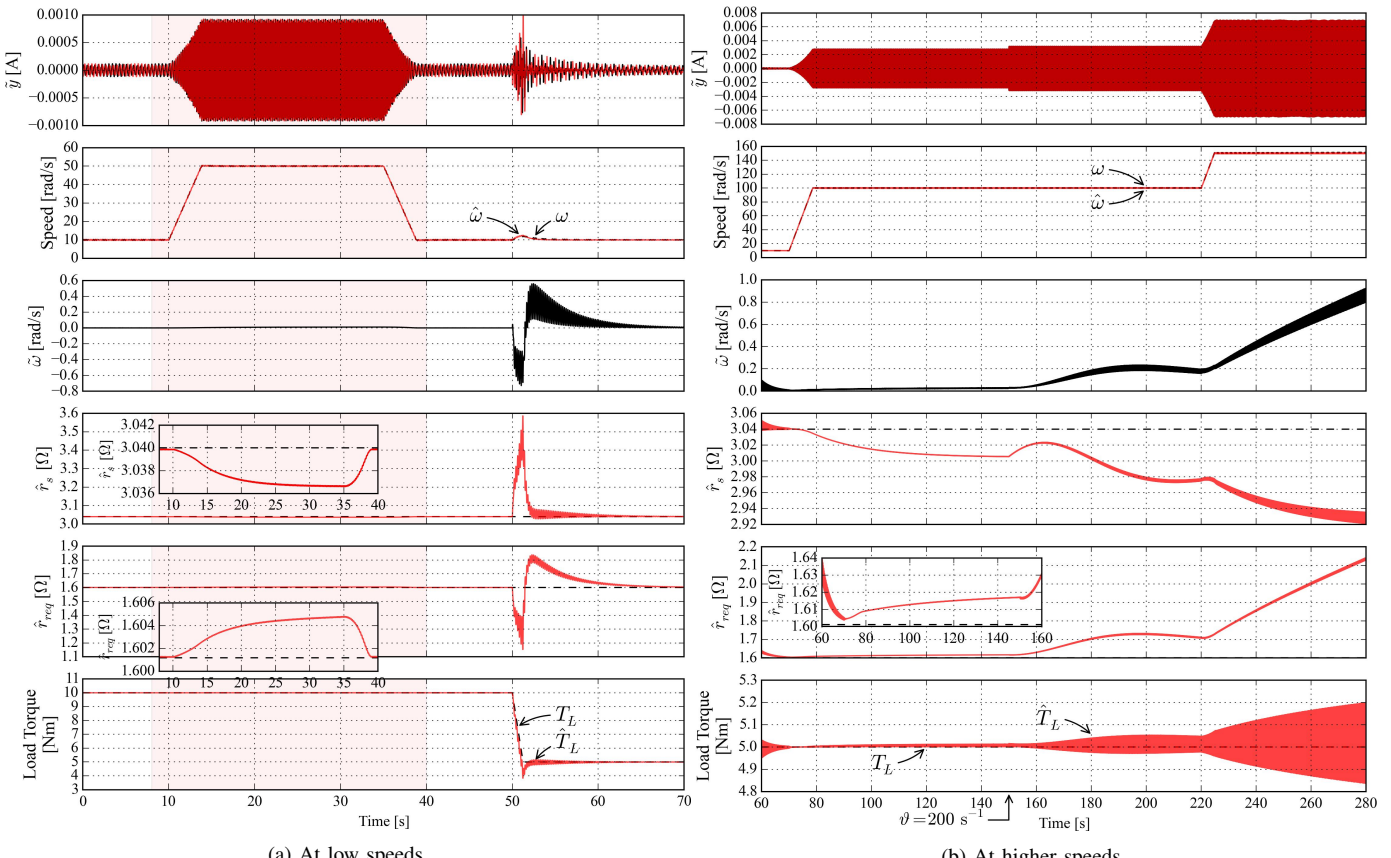


Fig. 1. Simulated sensorless control with resistances adaptation using the high gain AO. (When $t < 150$ s, $\vartheta = 100 \text{ s}^{-1}$.)

transient, the flux control never reaches a steady state. Considering this, Holtz and Quan's method is preferred in this paper.

B. Speed Estimation

The IM's motion equation based high gain speed observer shows extraordinary dynamic performance in simulation studies. Therefore, the motion equation is included in the proposed speed observer design.

1) Natural Speed Observer: The original implementation of the natural observer uses current model (CM) to estimate the rotor flux [36], [37]. By 'natural', it means the observer is an exact copy of the IM dynamics without any feedback terms. However, we find out that CM based flux estimation converges too slow. Its dynamic performance is inferior to VM based flux estimation, and it even causes stability issue in sensorless low speed regenerating operation.

With VM based flux estimate ψ_2 available, we propose the reduced-order natural speed observer based on the natural observer concept [37]

$$\begin{aligned} \hat{i}_{Ts} &= L_{\sigma}^{-1} \left[u_{Ts} - (\hat{r}_s + \hat{r}_{req}) \hat{i}_{Ts} - \hat{\omega} \psi_{M2} \right] \\ &\quad - \left(\hat{\omega} + \hat{r}_{req} \frac{i_s^T J \psi_2}{\psi_2^T \psi_2} \right) i_{Ms} \\ p\hat{\omega} &= \hat{J}_s^{-1} n_{pp} \left(n_{pp} \psi_{M2} \hat{i}_{Ts} - \hat{T}_L \right) \end{aligned} \quad (1)$$

where T_L is treated as a parameter, and quantities in the M - T frame are computed as follows

$$\begin{aligned} i_{Ms} &= i_{\alpha s} \cos \rho^* + i_{\beta s} \sin \rho^* \\ \psi_{M2} &= \psi_{\alpha 2} \cos \rho^* + \psi_{\beta 2} \sin \rho^* \\ u_{Ts} &= -u_{\alpha s} \sin \rho^* + u_{\beta s} \cos \rho^* \end{aligned} \quad (2)$$

with $\rho^* = \text{atan}(\psi_{\beta 2}, \psi_{\alpha 2})$. In fact, the reduced-order implementation is crucial for successful high speed operation. This is because tuning of \hat{T}_L only provides one degree-of-freedom to make either $u_s^T \hat{i}_s$ or $u_s^T \hat{J} \hat{i}_s$ converge to zero, not both (cf. [37]).

Obviously, the dynamic performance of the proposed speed observer depends on the knowledge of the estimated shaft inertia \hat{J}_s and estimated load torque \hat{T}_L . The adaptation rule for \hat{T}_L is driven by the estimated active power error $u_{Ts} \hat{i}_{Ts}$:

$$\begin{aligned} \hat{T}_L &= k_P \varepsilon + k_I \frac{1}{p} \varepsilon + k_D \dot{\varepsilon} \\ \varepsilon &= -\text{sgn}(u_{Ts}) u_{Ts} \hat{i}_{Ts} \\ \hat{i}_{Ts} &= -i_{\alpha s} \sin \rho^* + i_{\beta s} \cos \rho^* - \hat{i}_{Ts} \end{aligned} \quad (3)$$

in which, $k_P, k_I, k_D \in \mathbb{R}_+$.

2) Speed Estimation from the VM based Flux Estimation: The speed information can also be extracted from the VM based flux estimation as follows

$$\hat{\omega} = \frac{(J\psi_1)^T \dot{\psi}_1}{\psi_1^T \psi_1} - \hat{r}_{req} \frac{i_s^T J \psi_2}{\psi_2^T \psi_2} \quad (4)$$

where the computed stator flux ψ_1 and its time derivative $\dot{\psi}_1$ are given by

$$\begin{aligned}\psi_1 &= \psi_2 + L_\sigma i_s \\ \dot{\psi}_1 &= u_s - \hat{r}_s i_s\end{aligned}\quad (5)$$

The speed signal obtained from (4) can, of course, build a sensorless drive, but it is noisy in the experiment and its dynamic performance is no better than that of (1) if an accurate inertia value is provided. In this paper, (4) is only used for inertia identification.

C. Rotor Resistance Estimation

Rotor resistance determines how fast the flux modulus changes. Computing the derivative of $\|\psi_\mu\|^2$ yields

$$p\|\psi_\mu\|^2 = 2\psi_\mu^T p\psi_\mu = (-2\psi_\mu^T i_{req}) r_{req} \quad (6)$$

where $\psi_\mu^T i_{req}$ is the pseudo M -axis rotor current, and it is non-zero only when $\|\psi_\mu\|$ is time-varying. Based on this relation, a least mean square (LMS) model can be established exploiting the VM based flux estimation ψ_2 as follows [38]–[40]

$$\frac{p}{\tau_2 p + 1} \|\psi_2\|^2 = \frac{-2\psi_2^T i_2}{\tau_2 p + 1} \hat{r}_{req} \quad (7)$$

where $i_2 = L_\mu^{-1} \psi_2 - i_s$, and to avoid pure differentiation, the low-pass filter with τ_2 as its time constant is added. Please recall that the generation of ψ_2 is free of \hat{r}_{req} .

Based on the constant gain algorithm [39], the rotor resistance estimation in its discrete form is established as

$$\begin{aligned}\hat{r}_{req}[N] - \hat{r}_{req}[N-1] &= \frac{U[N]\gamma_{rreq}}{1+U[N]^2\gamma_{rreq}} \varepsilon_{rreq}[N] \\ \varepsilon_{rreq}[N] &= Y[N] - \hat{r}_{req}[N-1] U[N]\end{aligned}\quad (8)$$

where $U = \frac{-2}{\tau_2 p + 1} \psi_2^T i_2$, $Y = \frac{p}{\tau_2 p + 1} \|\psi_2\|^2$, $\gamma_{rreq} \in \mathbb{R}_+$, N is an integer.

In both simulation and experiment, dc offset in the pseudo M -axis rotor current ($\psi_2^T i_2$) is observed at steady state, which leads to speed-dependent r_{req} estimation. By intuition, this offset problem can be overcome by either of the two ideas. The first idea is to use Goertzel algorithm¹ to extract the ω_1 harmonics and then compute \hat{r}_{req} as follows

$$\begin{aligned}\hat{r}_{req}(t_{i+1}) &= \text{Goertzel}_{\omega_1}(Y)/\text{Goertzel}_{\omega_1}(U) \\ \hat{r}_{req}(t) &= \hat{r}_{req}(t_i), t \in [t_i, t_{i+1}], t_{i+1} = t_i + \frac{2\pi}{\omega_1}\end{aligned}\quad (9)$$

where function $\text{Goertzel}_{\omega_1}(\cdot)$ returns the amplitude of the input's ω_1 harmonic. This is only valid for speed steady-state and the estimate of r_{req} is updated every $\frac{2\pi}{\omega_1}$ seconds.

The other idea is to compensate the dc offset in the loop. That is, replace the signal U in (8) with the offset compensated version as follows

$$\begin{aligned}U &= \frac{-2}{\tau_2 p + 1} \psi_2^T i_2 - U_{\text{offset}} \\ U_{\text{offset}}(t_{i+1}) &= U_{\text{offset}}(t_i) + \sum_{N=t_i/T_s}^{t_{i+1}/T_s} U[N] \\ t_{i+1} &= t_i + \frac{2\pi}{\omega_1}\end{aligned}\quad (10)$$

with the sampling time T_s . The offset estimate U_{offset} is updated every $\frac{2\pi}{\omega_1}$ seconds, while the signal U is updated every T_s seconds.

¹Goertzel algorithm can be interpreted as a single tone detection version of FFT [41].

D. Stator Resistance Estimation

Stator resistance is crucial for motor operations near zero frequency, so a stator resistance estimation *that is exact at zero frequency* is desired. To this end, pre-multiplying the equation $r_s i_s = u_s - p\psi_s$ by i_s^T yields a steady-state least mean square model as follows

$$i_s^T i_s r_s = i_s^T u_s - \frac{\omega_\psi}{n_{pp}} (n_{pp} i_s^T J \psi_s) \quad (11)$$

which reads “stator heating loss equals stator input power minus power through air gap”. To avoid using ψ_2 that is related to \hat{r}_s , we propose the following adaptation rule for stator resistance using the constant gain algorithm [39]

$$\begin{aligned}\hat{r}_s[N] - \hat{r}_s[N-1] &= \frac{U[N]\gamma_{rs}}{1+U[N]^2\gamma_{rs}} \varepsilon_{rs} \\ \varepsilon_{rs} &= Y[N] - \hat{r}_s[N-1] U[N]\end{aligned}\quad (12)$$

where $U = i_s^T i_s$, $Y = i_s^T [u_s - J\omega_\psi (\psi_\mu^* + L_\sigma i_s)]$, $\gamma_{rs} \in \mathbb{R}_+$, N is an integer, and ψ_μ^* is the flux command transformed into the stationary α - β frame. Since time-varying flux modulus command ψ^* contains an ω_1 -component, we should modify the adaptation rule (12) using hybrid update law [42], [43].

E. Shaft Inertia Estimation in a Sensorless Drive

Speed estimation based on the IM motion equation relies on the shaft inertia J_s . However, most inertia identification methods rely on the speed signal (see e.g., [44], [45]). Therefore, in our sensorless drive, we propose to use the speed signal $\hat{\omega}$ obtained from (4) instead, which is free of the information of J_s . Particularly, we adopt the well-known orthogonality based inertia identification method by Awaya *et al.* [46] and alter it for a sensorless drive.

First, Awaya *et al.* [46] assume the speed signal is periodical such that $\hat{\omega}(t + \tau_p) = \hat{\omega}(t), \forall t > 0$ with τ_p the period. However, in the experiment, the estimated speed from (4) is contaminated by noises of large magnitudes, because the stator voltage u_s is directly used in (4). As a result, the signal $\hat{\omega}(t)$ is not a periodical signal. To reconstruct a periodical signal out of $\hat{\omega}$, we introduce

$$\varpi = \frac{1}{\tau_4 p + 1} \hat{\omega} \quad (13)$$

where $\tau_4 \in \mathbb{R}_+$, and the tuning principle of τ_4 is to make the reconstructed signal ϖ a periodical signal such that $\varpi(t + \tau_p) = \varpi(t), \forall t > 0$.

Then, we construct an estimate of the load torque (denoted by T_{est}) as follows (see Appendix for details)

$$T_{\text{est}} = \frac{1}{\tau_5 p + 1} \hat{T}_{\text{em}} - J_{sN} \frac{p}{\tau_5 p + 1} \frac{\hat{\omega}}{n_{pp}} \quad (14)$$

where J_{sN} is the nominal value of J_s , τ_5 is the time constant of the filters, and $\hat{T}_{\text{em}} = n_{pp} i_s^T J \psi_2$ is the computed electromagnetic torque.

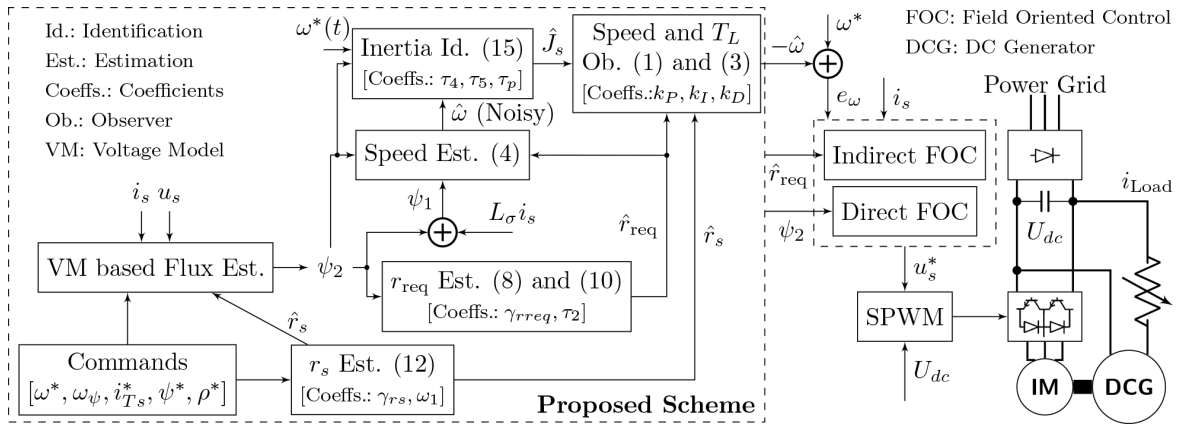


Fig. 2. Block diagram of the proposed scheme and the experimental system setup.

Finally, with the aid of the signal \dot{q}_1 given by $\dot{q}_1 = -\tau_5^{-1}q_1 + \tau_5^{-1}\varpi/n_{pp}$ with $q_1|_{t=0} = 0$, the estimated variation in J_s is computed by

$$\Delta J_s = \lim_{k \rightarrow \infty} \frac{\int_{(k-1)\tau_p}^{k\tau_p} \dot{q}_1 \left(\frac{1}{\tau_{ap+1}} T_{est} \right) dt}{\int_{(k-1)\tau_p}^{k\tau_p} \dot{q}_1 \dot{q}_1 dt}, \quad k = 1, 2, \dots \quad (15)$$

where τ_p is the period of the speed signal ϖ . Finally, the estimate of J_s is computed by $\hat{J}_s = J_{sN} + \Delta J_s$.

F. Brief Summary

To show the relations among all methods introduced in this section, a block diagram is sketched in Fig. 2, from which we should emphasize that all the parameter identifiers are independent of the output of the speed observer. Particularly, \hat{r}_s is first obtained from voltage, current and commands. Upon \hat{r}_s , ψ_2 is reconstructed as the basis for r_{req} as well as J_s identification. In other words, the proposed scheme eliminates two-way coupling among parameters and speed, as compared to its AO counterpart.

The stability analysis of the load torque adaptive speed observer (1) and (3) are given in Appendix B, whereas the stability analysis of the whole inter-connected system is open.

III. EXPERIMENTAL VALIDATION

A. System Setup

The nameplate data of the tested IM are 4 kW, 1440 rpm, 380 Vrms and 8.8 Arms. The nominal values of the IM parameters are listed in Table I. The load torque is provided by a separately excited dc generator. Particularly, the regenerative load torque is produced by connecting the armature of the dc generator to the dc bus, as shown in Fig. 2.

An encoder is equipped for verification purpose, and with the aid of the measured speed, we reconstruct the rotor flux signal and the load torque signal using the reduced-order flux observer and the second-order load torque estimator described in [47, Eq.(3.33),(3.84)]. Please note that the nominal values of parameters are used, which means that the reconstructed signals could not exactly comply with the actual ones. However, for the sake of concise notation, we still designate the reconstructed signals by $\psi_\mu = [\psi_{\alpha\mu} \psi_{\beta\mu}]^T$ and T_L . They are

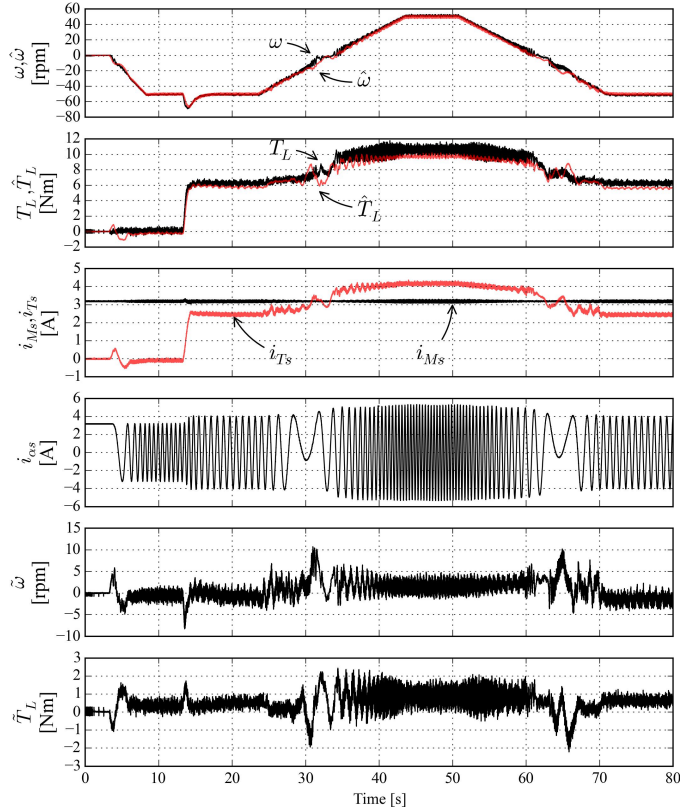


Fig. 3. Sensorless slow speed reversal. T_L is reconstructed using ω [47, Eq.(3.84)].

only for verification purpose. In all experiments, the observed speed $\hat{\omega}$ from the natural speed observer (1) is used for control.

As for inductance parameters, the magnetizing inductance L_μ is looked up by an off-line identified magnetizing curve using $\|\psi_2\|$, while the leakage inductance L_σ is set to its nominal value. Discussion of uncertainty effects of L_μ and L_σ are available in [13] and [11], respectively.

B. Slow Speed Reversal

To show the natural speed observer's effectiveness near zero frequency, the sensorless slow speed reversal test [5] is first performed and its results are recorded in Fig. 3. During this

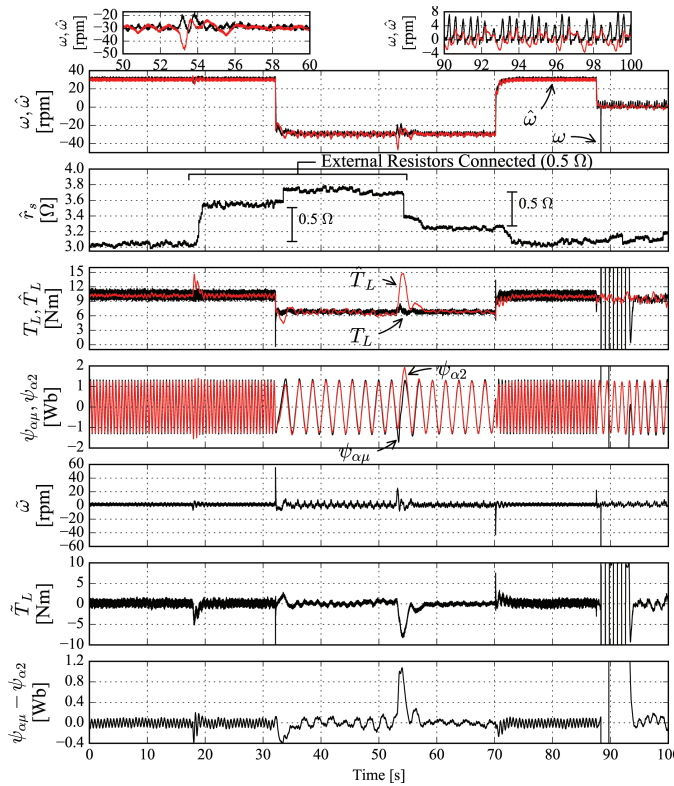


Fig. 4. Low speed sensorless fast speed reversal between motoring and regenerating operations. $\psi_{\alpha\mu}$ and T_L are reconstructed using ω [47, Eq.(3.33),(3.84)].

test, \hat{r}_s and \hat{r}_{req} are fixed to their nominal values, considering the following two facts. For one thing, the proposed stator resistance estimation method is only valid at steady state. For another, based on our simulation and experiment studies, the rotor resistance estimation using ψ_2 highly depends on the accuracy of the stator resistance at low speeds. In effect, error in \hat{r}_s drives \hat{r}_{req} towards 0 to certain extent.

The successful slow speed reversal tests demonstrates the effectiveness of using ψ_2 in the natural speed observer. However, it is seen that the estimated load torque is slightly biased. This is because of the detuned stator resistance.

C. Low Speed Regenerating & Motoring Operation

The results of the sensorless control at low speeds are shown in Fig. 4. The fast speed reversal is applied at $t = 32$ s and $t = 70$ s to test the dynamic performance of the proposed drive with a nominal inertia value $\hat{J}_s = J_{sN} = 0.017 \text{ kgm}^2$, which does not equal to J_s . It is found that an erroneous inertia value does not cause stability issues. One observes that the proposed drive can operate stably during both motoring and regenerating operations. Regeneration mode is the motor operation in which speed and torque have different signs [5].

The motor speed has two kinds of side effects on the stator resistance estimate (\hat{r}_s), i.e., speed oscillation and working conditions. Since the stator resistance identifier uses a simplified steady state model, if speed oscillates under a constant speed command, the estimate \hat{r}_s will also oscillate. This phenomenon is especially apparent when the zero speed

command is applied in Fig. 4 after $t = 87.5$ s when the speed oscillation is severe.

The motor working condition is closely related to the speed. Since the load torque is positive in Fig. 4, the positive speed changing to a negative value will make the motor leaving motoring operation and entering regenerating operation. Even though \hat{r}_s converges to different values for motoring and regenerating operations,² the load torque estimation accuracy and the speed estimation accuracy are seen to be improved, compared to the results of Fig. 3 with a fixed \hat{r}_s .

To further show the effectiveness of the proposed stator resistance estimation method, we connect/remove the external resistors (0.5Ω) to/from the stator windings at $t = 18.5/54.5$ s. The increment in \hat{r}_s after the external resistors are connected is exactly 0.5Ω regardless of the operating conditions.

After $t = 87.5$ s, zero speed operation is realized. It is interesting to point out that a spike arises in the measured speed ω at $t = 88.3$ s. This speed spike is due to a hardware issue of the test bench. Specifically, only the A+, B+, Z+ signals from the encoder are exploited, while the A-, B-, Z- signals are simply ignored. As a result, the encoder signals could easily be disturbed by inverter's electromagnetic interference. As a result, the reconstructed signals $\psi_{\alpha\mu}$ and T_L that use ω are drastically disturbed. The disturbed signals go back to normal after the spike in the measured speed disappears for several seconds, while the sensorless system is not influenced at all.

D. Sensorless Identification of Inertia and Rotor Resistance

In Fig. 5, the proposed sensorless inertia identification is tested under a periodical speed command. It can be seen that the noises in $\hat{\omega}$ [obtained from (4)] are almost eliminated by the filter $\frac{1}{\tau_{4p+1}}$, resulting in a severely delayed ϖ w.r.t. $\hat{\omega}$. Even though, it is observed that inertia can be fast identified within 2 cycles from the filtered signal ϖ .

In an another speed-sensored inertia identification test, we use the electromagnetic torque that is computed by the reconstructed ψ_μ , along with the measured speed ω , to implement the speed-sensored inertia identification counterpart [46]. The steady-state averaged value of the estimated inertia value from this test is $J_s = 0.063 \text{ kgm}^2$, which means the normalized estimated error for the sensorless inertia identification test is 1.6%, as shown in the zoomed-in plot in Fig. 5.

In addition, thanks to the injected ω_1 -component in flux modulus command ψ^* (see Table I), it is possible to identify rotor resistance in the meantime. The sensorless inertia identification is dependent on \hat{r}_{req} [see (4)]. However, it is found in the experiment, the proposed sensorless inertia identification is not sensitive to variation in \hat{r}_{req} in no-load conditions in which slip is near null.

E. Response to Step Speed Command

In Fig. 6, the experimental results of the step responses of the proposed drive are presented. Different inertia values

²One possible reason is that the inverter has different values for its equivalent on-state resistance during motoring and regenerating operations when the active power or real power changes its sign.

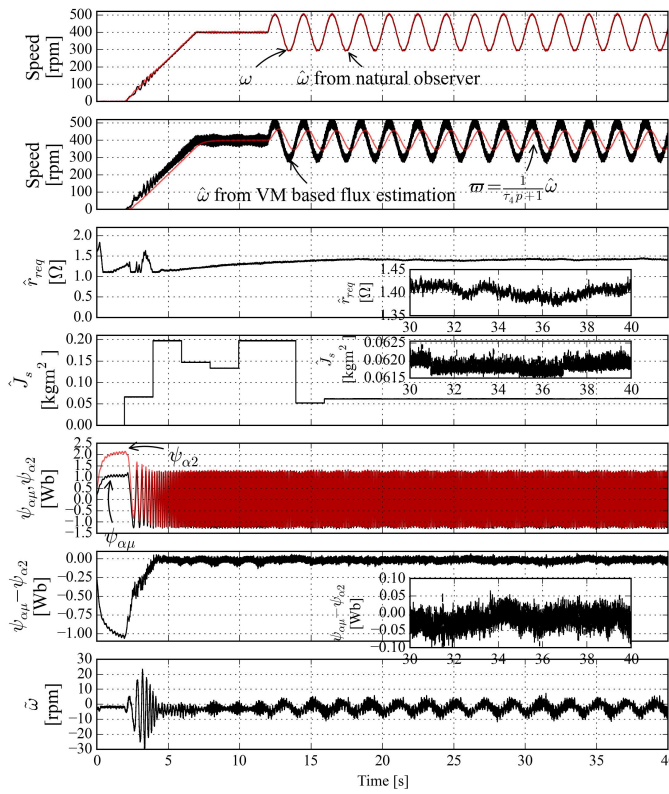


Fig. 5. Medium speed sensorless control under biased sinusoidal speed command with inertia and rotor resistance identification. $\psi_{\alpha\mu}$ is reconstructed using ω [47, Eq.(3.33)].

are used: J_s , $0.5J_s$ and $1.5J_s$ (in time order). The first step response using $\hat{J}_s = J_s$ gives the smallest spikes in speed estimated error $\tilde{\omega}$ and almost no spikes in \hat{T}_L during transients. On the other hand, an over-estimated inertia value $\hat{J}_s = 1.5J_s$ results in the largest spikes in $\tilde{\omega}$ and \hat{T}_L during transients and an oscillated \hat{T}_L profile at high speed steady state, which further leads to oscillation in speed, as shown in the zoomed-in plots on the top of Fig. 6. Even though oscillation exists in speed, it is observed that $\tilde{\omega}$ still tracks the profile of ω , rather than being a low-pass filtered version or a noise-contaminated version of ω . Overall, the results confirm that using the motion equation of IM has the potential of good dynamic performance for speed estimation [36].

As for the rotor resistance estimation, it is crucial that our proposed offset compensation is used, or else a speed-dependent rotor resistance estimation is expected. From Fig. 6, it is noticed that a larger offset U_{offset} in signal U needs to be compensated at higher speed. However, during the speed transients, the offset compensation U_{offset} can become erroneous, which leads to disturbed rotor resistance estimation. Overall, our proposed sensorless scheme with a pre-identified inertia value exhibits good dynamic performance.

F. High Speed Reversal Test

In Fig. 7, the results of the sensorless high speed reversal are presented. The proposed natural speed observer tracks the actual speed well even during speed transients. It takes about 2.2 s for the motor to go from +1500 rpm to -1500 rpm,

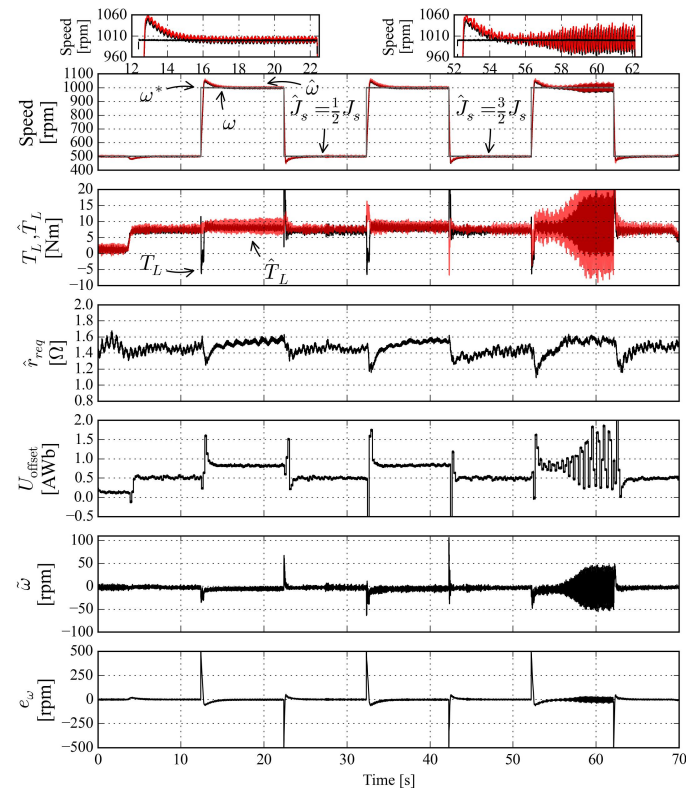


Fig. 6. Step responses of the sensorless control with rotor resistance identification. The speed control error e_ω is defined by $e_\omega = \omega^* - \tilde{\omega}$.

which means the acceleration is around 1363 rpm/s with a current limit of 10 A for i_{Ts} . Note that torque current i_{Ts} is saturated during the speed transients, which implies that the dynamic performance can become faster if over-current is allowed. Besides, the M -axis current can also be tuned along with the magnetizing inductance curve to obtain the maximal torque output out of the motor.

Again, the detuned offset compensation U_{offset} deteriorates the rotor resistance estimation during the speed reversal transients. However, the rotor resistance quickly converges even during the speed reversal as long as the disturbance in U_{offset} disappear. The steady state value of U_{offset} at 1500 rpm is 2 AWb, which is larger than the values of U_{offset} in Fig. 6 at 500 rpm and 1000 rpm. This confirms the necessity and effectiveness of the proposed offset compensation for the rotor resistance estimation, to produce a speed-independent rotor resistance estimate.

IV. CONCLUSION

After showing the low parameter sensitivity problem of the cutting-edge high gain AO, this paper presents an alternative solution to compensate parameters uncertainties in sensorless IM drives. The conclusion is that using one AO estimating all the unmeasured states and uncertain parameters is mostly of theoretical interest, while the proposed alternative scheme shows its practical significance for being capable of achieving dynamic speed estimation as well as separately tuned resistances estimations. The proposed scheme removes two-way coupling among parameters and speed, and meanwhile it

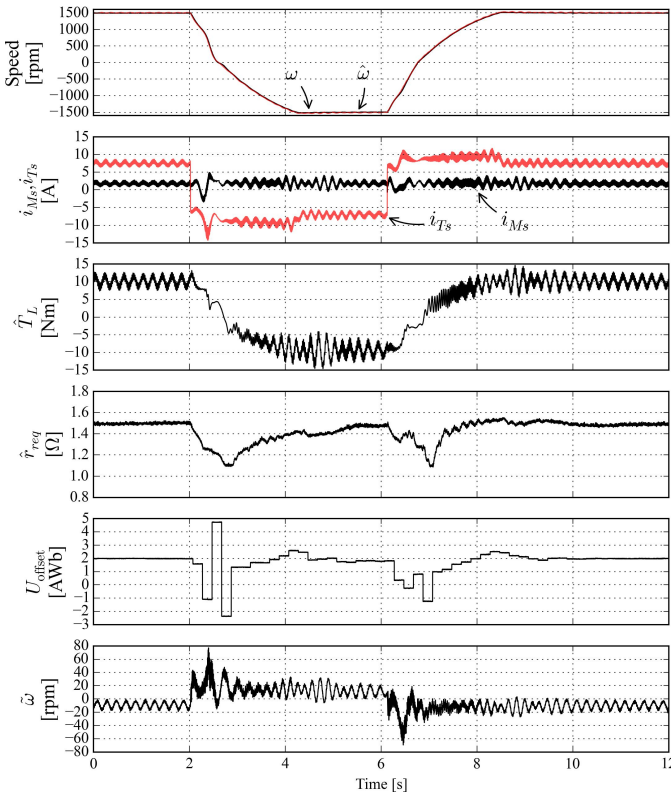


Fig. 7. Sensorless high speed reversal with rotor resistance identification.

consumes less computational resources, showing the potential to be implemented for cheaper chips. Main contributions of this paper are: i) to extend the operating range of the natural speed observer [37], ii) to overcome the speed-dependent rotor resistance estimation problem reported in [40], iii) to identify shaft inertia in a sensorless drive, and (iv) to propose a complete scheme for practical implementation of an adaptive sensorless drive.

APPENDIX

A. DEDUCTION OF ΔJ_s IDENTIFICATION RULE (15)

Several assumptions are made first:

- (1) Estimated speed $\hat{\omega} = \omega + \text{Noise}$ but $\varpi = \frac{1}{\tau_{4p+1}}\omega$ with a proper τ_4 is periodical. This implies that noises are eliminated, i.e., $\frac{1}{\tau_{4p+1}}\text{Noise} \approx 0$.
- (2) The load torque could be described by $T_L = D\frac{\omega}{n_{pp}} + T_C$, where D is the viscous coefficient and T_C is the constant part of T_L .
- (3) The computed electromagnetic torque is accurate, i.e., $\hat{T}_{em} = T_{em}$.

From IM's motion equation: $\frac{J_s}{n_{pp}}p\omega = T_{em} - T_L$, we construct an estimate of the load torque (denoted by T_{est}) using Gopinath's reduced-order observer [48] as follows

$$\begin{aligned} pT_{est} &= \tau_5^{-1}(y_{eq} - T_{est}) \\ &= \tau_5^{-1}\left(\hat{T}_{em} - \frac{J_{sN}}{n_{pp}}p\hat{\omega} - T_{est}\right) \end{aligned} \quad (16)$$

with the equivalent (load torque) output y_{eq} . Then, introduce the intermediate variable ζ to avoid differentiation:

$$\zeta = \tau_5 T_{est} + \frac{J_{sN}}{n_{pp}}\hat{\omega} \quad (17)$$

whose dynamics are

$$\begin{aligned} p\zeta &= \hat{T}_{em} - T_{est} = \hat{T}_{em} - \tau_5^{-1}\zeta + \tau_5^{-1}\frac{J_{sN}}{n_{pp}}\hat{\omega} \\ \Rightarrow \zeta &= \frac{1}{p + \tau_5^{-1}}\left(\hat{T}_{em} + \tau_5^{-1}\frac{J_{sN}}{n_{pp}}\hat{\omega}\right) \end{aligned} \quad (18)$$

Note that (14) is derived using (17) and (18). In turn, we can derive the dynamics of T_{est}

$$\begin{aligned} pT_{est} &= \tau_5^{-1}\dot{\zeta} - \tau_5^{-1}\frac{J_{sN}}{n_{pp}}p\hat{\omega} \\ \Rightarrow T_{est} &= \frac{1}{\tau_5 p + 1}\left(D\frac{\omega}{n_{pp}} + T_C + \frac{\Delta J_s}{n_{pp}}p\hat{\omega}\right) \end{aligned} \quad (19)$$

Filtering both sides of (19) with $\frac{1}{\tau_{4p+1}}$ yields

$$\begin{aligned} \frac{T_{est}}{\tau_{4p+1}} &= \frac{1}{\tau_5 p + 1}\left(\frac{D}{n_{pp}}\varpi + \frac{1}{\tau_{4p+1}}T_C + \frac{\Delta J_s}{n_{pp}}p\varpi\right) \\ &\triangleq Dq_1 + \frac{1}{\tau_{4p+1}}q_2 T_C + \Delta J_s \dot{q}_1 \end{aligned} \quad (20)$$

with $\dot{q}_2 = -\tau_5^{-1}q_2 + \tau_5^{-1}$, $\dot{q}_1 = -\tau_5^{-1}q_1 + \tau_5^{-1}\varpi/n_{pp}$.

Owing to the orthogonality among the signals q_1, \dot{q}_1, q_2 , we have [46]:

$$\lim_{N \rightarrow \infty} \int_{(N-1)\tau_p}^{N\tau_p} q_1 \dot{q}_1 dt = \lim_{N \rightarrow \infty} \int_{(N-1)\tau_p}^{N\tau_p} q_2 \dot{q}_1 dt = 0 \quad (21)$$

Consequently, (15) is deduced using (20) and (21).

B. STABILITY ANALYSIS OF LOAD TORQUE ADAPTIVE SPEED OBSERVER (1) AND (3)

Several assumptions are made as follows.

- The flux estimate ψ_2 is consistent with the actual flux ψ_μ . Consequently, the M -axis of the $M-T$ frame is aligned with the actual rotor flux vector.
- The parameters (i.e., r_s , r_{req} and J_s) are known.
- The load torque T_L is constant, i.e., $pT_L = 0$.

As a result, the original nonlinear error dynamics are reduced to the linear ones as $px = Ax$, with $x = [\tilde{i}_{Ts}, \hat{\omega}, \tilde{T}_L]^T$ and A defined as follows

$$A = \begin{bmatrix} -L_\sigma^{-1}(r_s + r_{req}) & -(i_{Ms} + L_\sigma^{-1}\psi_{M2}) & 0 \\ 0 & 0 & -J_s^{-1}n_{pp} \\ |u_{Ts}| \left(k_I - k_P \frac{r_s + r_{req}}{L_\sigma}\right) & -k_P |u_{Ts}| (L_\sigma^{-1}\psi_{M2} + i_{Ms}) & 0 \end{bmatrix} \quad (22)$$

Note that such linear system consists of time-varying parameters that are actual states/inputs for the original system, such as ψ_{M2} , i_{Ms} and u_{Ts} . Consider a Lyapunov function candidate $U(x, t)$

$$U = (Ax)^T Ax > 0 \quad (23)$$

whose time derivative along error dynamics \dot{x} is

$$\dot{U} = x^T A^T (A^T + A) Ax < 0 \quad (24)$$

If (23) and (24) hold, $U(x, t)$ is a Lyapunov function. To this end, one should first choose k_P to satisfy

$$k_P < \frac{-J_s^{-1}n_{pp}}{|u_{Ts}|(L_\sigma^{-1}\psi_{M2} + i_{Ms})} \quad (25)$$

$$\Rightarrow -J_s^{-1}n_{pp} - k_P |u_{Ts}|(L_\sigma^{-1}\psi_{M2} + i_{Ms}) = C > 0$$

and then choose k_I to satisfy

$$k_I > k_P \frac{r_s + r_{req}}{L_\sigma} + C \frac{L_\sigma^{-1}(r_s + r_{req})}{(i_{Ms} + L_\sigma^{-1}\psi_{M2})|u_{Ts}|} \quad (26)$$

This is a sufficient condition for the error dynamics $\dot{x} = Ax$ having asymptotical stability about the origin $x = 0$.

REFERENCES

- [1] J. Holtz, "Sensorless control of induction motor drives," *Proceedings of the IEEE*, vol. 90, no. 8, pp. 1359–1394, Aug 2002.
- [2] H. Toliyat, E. Levi, and M. Rainia, "A review of rfo induction motor parameter estimation techniques," *Energy Conversion, IEEE Transactions on*, vol. 18, no. 2, pp. 271–283, June 2003.
- [3] J. Chen and J. Huang, "Stable simultaneous stator and rotor resistances identification for speed sensorless im drives: Review and new results," *IEEE Transactions on Power Electronics*, vol. 33, no. 10, pp. 8695–8709, Oct 2018.
- [4] L. Harnefors, "Globally stable speed-adaptive observers for sensorless induction motor drives," *IEEE Transactions on Industrial Electronics*, vol. 54, no. 2, pp. 1243–1245, April 2007.
- [5] L. Harnefors and M. Hinkkanen, "Stabilization methods for sensorless induction motor drives — a survey," *IEEE Journal of Emerging and Selected Topics in Power Electronics*, vol. 2, no. 2, pp. 132–142, June 2014.
- [6] C. Schauder, "Adaptive speed identification for vector control of induction motors without rotational transducers," *Industry applications, IEEE Transactions on*, vol. 28, no. 5, pp. 1054–1061, 1992.
- [7] A. Pavlov and A. Zaremba, "Adaptive observers for sensorless control of an induction motor," in *Proceedings of the 2001 American Control Conference. (Cat. No.01CH37148)*, vol. 2, 2001, pp. 1557–1562 vol.2.
- [8] A. Dib, M. Farza, M. M'Saad, P. Dorleans, and J.-F. Massieu, "High gain observer for sensorless induction motor," *IFAC Proceedings Volumes*, vol. 44, no. 1, pp. 674–679, 2011.
- [9] S. Solvar, M. Ghanes, L. Amet, J.-P. Barbot, and G. Santomenna, "Industrial application of a second order sliding mode observer for speed and flux estimation in sensorless induction motor," in *Induction Motors*, P. R. E. Araújo, Ed. Rijeka: IntechOpen, 2012, ch. 15. [Online]. Available: <https://doi.org/10.5772/52910>
- [10] M. Farza, M. M'Saad, T. Ménard, A. Ltaief, and T. Maatoug, "Adaptive observer design for a class of nonlinear systems. application to speed sensorless induction motor," *Automatica*, vol. 90, pp. 239–247, 2018.
- [11] J. Chen and J. Huang, "Globally stable speed-adaptive observer with auxiliary states for sensorless induction motor drives," *IEEE Transactions on Power Electronics*, vol. 34, no. 1, pp. 33–39, Jan 2019.
- [12] J. Chen, J. Huang, and Y. Sun, "Resistances and speed estimation in sensorless induction motor drives using a model with known regressors," *IEEE Transactions on Industrial Electronics*, vol. 66, no. 4, pp. 2659–2667, April 2019.
- [13] J. Chen and J. Huang, "Application of adaptive observer to sensorless induction motor via parameter-dependent transformation," *IEEE Transactions on Control Systems Technology*, vol. 27, no. 6, pp. 2630–2637, Nov 2019.
- [14] Z. Yan, C. Jin, and V. Utkin, "Sensorless sliding-mode control of induction motors," *IEEE Transactions on Industrial Electronics*, vol. 47, no. 6, pp. 1286–1297, Dec 2000.
- [15] H. K. Khalil and E. G. Strangas, "Sensorless speed control of induction motors," in *Proceedings of the 2004 American Control Conference*, vol. 2, June 2004, pp. 1127–1132 vol.2.
- [16] H. K. Khalil, E. G. Strangas, and S. Jurkovic, "Speed observer and reduced nonlinear model for sensorless control of induction motors," *IEEE Transactions on Control Systems Technology*, vol. 17, no. 2, pp. 327–339, March 2009.
- [17] M. Montanari, S. M. Peresada, C. Rossi, and A. Tilli, "Speed sensorless control of induction motors based on a reduced-order adaptive observer," *IEEE Transactions on Control Systems Technology*, vol. 15, no. 6, pp. 1049–1064, Nov 2007.
- [18] R. Marino, P. Tomei, and C. M. Verrelli, "An adaptive tracking control from current measurements for induction motors with uncertain load torque and rotor resistance," *Automatica*, vol. 44, no. 10, pp. 2593–2599, 2008.
- [19] A. Dib, "Sensorless indirect adaptive control with parameters and load-torque estimation of induction motor," in *CCCA12*, Dec 2012, pp. 1–6.
- [20] M. Ghanes and G. Zheng, "On sensorless induction motor drives: Sliding-mode observer and output feedback controller," *IEEE Transactions on Industrial Electronics*, vol. 56, no. 9, pp. 3404–3413, Sept 2009.
- [21] M. Ghanes, J.-B. Barbot, J. D. Leon, and A. Glumineau, "A robust sensorless output feedback controller of the induction motor drives: new design and experimental validation," *International Journal of Control*, vol. 83, no. 3, pp. 484–497, 2010. [Online]. Available: <https://doi.org/10.1080/00207170903193474>
- [22] Y. Xu, C. Morito, and R. D. Lorenz, "Extending high-speed operating range of induction machine drives using deadbeat-direct torque and flux control with precise flux weakening," *IEEE Transactions on Industry Applications*, 2019.
- [23] Y. Xu, Y. Wang, R. Iida, and R. D. Lorenz, "Extending low-speed self-sensing via flux tracking with volt-second sensing," *IEEE Transactions on Industry Applications*, vol. 54, no. 5, pp. 4405–4414, 2018.
- [24] G. Lefebvre, J. Y. Gauthier, A. Hijazi, X. Lin-Shi, and V. L. Digarcher, "Observability-index-based control strategy for induction machine sensorless drive at low speed," *IEEE Transactions on Industrial Electronics*, vol. 64, no. 3, pp. 1929–1938, March 2017.
- [25] M. Korzonek, G. Tarchala, and T. Orlowska-Kowalska, "A review on mras-type speed estimators for reliable and efficient induction motor drives," *ISA transactions*, 2019.
- [26] L. Zhao, J. Huang, H. Liu, B. Li, and W. Kong, "Second-order sliding-mode observer with online parameter identification for sensorless induction motor drives," *Industrial Electronics, IEEE Transactions on*, vol. 61, no. 10, pp. 5280–5289, 2014.
- [27] H. Wang, X. Ge, and Y. Liu, "Second-order sliding-mode mras observer-based sensorless vector control of linear induction motor drives for medium-low speed maglev applications," *IEEE Transactions on Industrial Electronics*, vol. 65, no. 12, pp. 9938–9952, Dec 2018.
- [28] R. Marino, T. Patrizio, and M. C. Verrelli, *AC Electric Motors Control: Advanced Design Techniques and Applications*. Wiley Online Library, 2013, ch. Adaptive Output Feedback Control of Induction Motors, pp. 158–187.
- [29] C. Verrelli, P. Tomei, E. Lorenzani, R. Fornari, and F. Immovilli, "Further results on nonlinear tracking control and parameter estimation for induction motors," *Control Engineering Practice*, vol. 66, pp. 116 – 125, 2017. [Online]. Available: <http://www.sciencedirect.com/science/article/pii/S0967066117301247>
- [30] C. Mastorocostas, I. Kioskeridis, and N. Margaris, "Thermal and slip effects on rotor time constant in vector controlled induction motor drives," *IEEE Transactions on Power Electronics*, vol. 21, no. 2, pp. 495–504, March 2006.
- [31] A. Dib, "Observation et commande de la machine asynchrone," Ph.D. dissertation, Université de Caen, 2012.
- [32] J. Chen, J. Huang, and M. Ye, "Totally adaptive observer for speed sensorless induction motor drives: Simply a cost of extra energy consumption," in *2017 IEEE International Electric Machines and Drives Conference (IEMDC)*, May 2017, pp. 1–7.
- [33] D. Stojić, M. Milinković, S. Veinović, and I. Klasnić, "Improved stator flux estimator for speed sensorless induction motor drives," *IEEE Transactions on Power Electronics*, vol. 30, no. 4, pp. 2363–2371, April 2015.
- [34] T. Ohtani, "Reduction of motor parameter sensitivity in vector-controlled induction motor without shaft encoder," *IEEJ Transactions on Industry Applications*, vol. 110, no. 5, pp. 497–505, 1990.
- [35] J. Holtz and J. Quan, "Drift- and parameter-compensated flux estimator for persistent zero-stator-frequency operation of sensorless-controlled induction motors," *IEEE Transactions on Industry Applications*, vol. 39, no. 4, pp. 1052–1060, July 2003.
- [36] J. Maes and J. A. Melkebeek, "Speed-sensorless direct torque control of induction motors using an adaptive flux observer," *IEEE Transactions on Industry Applications*, vol. 36, no. 3, pp. 778–785, May 2000.
- [37] S. R. Bowes, A. Sevinc, and D. Holliday, "New natural observer applied to speed-sensorless dc servo and induction motors," *IEEE Transactions on Industrial Electronics*, vol. 51, no. 5, pp. 1025–1032, Oct 2004.
- [38] T. Kanmachi and I. Takahashi, "Sensorless speed control of an induction motor with no influence of resistance variation," in *Power Conversion Conference - Nagaoka 1997., Proceedings of the*, vol. 1, Aug 1997, pp. 91–96 vol.1.

- [39] K. Akatsu and A. Kawamura, "Online rotor resistance estimation using the transient state under the speed sensorless control of induction motor," *IEEE Transactions on Power Electronics*, vol. 15, no. 3, pp. 553–560, May 2000.
- [40] ——, "Sensorless very low-speed and zero-speed estimations with online rotor resistance estimation of induction motor without signal injection," *Industry Applications, IEEE Transactions on*, vol. 36, no. 3, pp. 764–771, 2000.
- [41] M. Carraro and M. Zigliotto, "Automatic parameter identification of inverter-fed induction motors at standstill," *IEEE Transactions on Industrial Electronics*, vol. 61, no. 9, pp. 4605–4613, Sept 2014.
- [42] J. Chen and J. Huang, "Online decoupled stator and rotor resistances adaptation for speed sensorless induction motor drives by a time-division approach," *IEEE Transactions on Power Electronics*, vol. 32, no. 6, pp. 4587–4599, June 2017.
- [43] S. Sastry and M. Bodson, *Adaptive control: stability, convergence and robustness*. Prentice-Hall, Inc., 1989.
- [44] R. Garrido and A. Concha, "Inertia and friction estimation of a velocity-controlled servo using position measurements," *IEEE Transactions on Industrial Electronics*, vol. 61, no. 9, pp. 4759–4770, Sept 2014.
- [45] Y. Zuo, X. Zhu, L. Quan, C. Zhang, Y. Du, and Z. Xiang, "Active disturbance rejection controller for speed control of electrical drives using phase-locking loop observer," *IEEE Transactions on Industrial Electronics*, vol. 66, no. 3, pp. 1748–1759, 2019.
- [46] I. Awaya, Y. Kato, I. Miyake, and M. Ito, "New motion control with inertia identification function using disturbance observer," in *Proceedings of the 1992 International Conference on Industrial Electronics, Control, Instrumentation, and Automation*, Nov 1992, pp. 77–81 vol.1.
- [47] R. Marino, P. Tomei, and C. M. Verrelli, *Induction motor control design*. Springer London, 2010.
- [48] B. Gopinath, "On the control of linear multiple input-output systems," *Bell System Technical Journal*, vol. 50, no. 3, pp. 1063–1081, 1971. [Online]. Available: <http://dx.doi.org/10.1002/j.1538-7305.1971.tb01896.x>



Jiahao Chen (S'17–M'19) received the B.Sc. degree in electrical engineering from Zhejiang University, China, in 2014, where he is currently pursuing the Ph.D. degree in electrical engineering with the College of Electrical Engineering. Since September 2018, he was a visiting scholar at the University of Wisconsin-Madison, USA for one year, where he was involved in bearingless motors.

His research interests include self-sensing techniques and parameter estimation of electric machines, with a special focus on the stable adaptive observer design.



Jin Huang received the B.Sc. degree in electrical engineering from Zhejiang University, Hangzhou, China, in 1982, and the Ph.D. degree in electrical engineering from the National Polytechnic Institute of Toulouse, Toulouse, France, in 1987. From 1987 to 1994, he was an Associate Professor with the College of Electrical Engineering, Zhejiang University. Since 1994, he has been a Professor at Zhejiang University.

His research interests include electrical machine, ac drives, multiphase machine, and motor parameter identification.